

Invariant texture analysis through Local Binary Patterns

Rodrigo Nava^a, Gabriel Cristóbal^b, Boris Escalante-Ramírez^c

^a*Posgrado en Ciencia e Ingeniería de la Computación, Universidad Nacional Autónoma de México, Mexico City, Mexico*

^b*Instituto de Óptica, Serrano 121, 28006 Madrid, Spain*

^c*Facultad de Ingeniería, Universidad Nacional Autónoma de México, Mexico City, Mexico*

Abstract

In many image processing applications, such as segmentation and classification, the selection of robust features descriptors is crucial to improve the discrimination capabilities in real world scenarios. In particular, it is well known that image textures constitute power visual cues for feature extraction and classification. In the past few years the local binary pattern (LBP) approach, a texture descriptor method proposed by Ojala et al., has gained increased acceptance due to its computational simplicity and more importantly for encoding a powerful signature for describing textures. However, the original algorithm presents some limitations such as noise sensitivity and its lack of rotational invariance which have led to many proposals or extensions in order to overcome such limitations. In this paper we performed a quantitative study of the Ojala's original LBP proposal together with other recently proposed LBP extensions in the presence of rotational, illumina-

Email addresses: urielrnv@uxmcc2.iimas.unam.mx (Rodrigo Nava), gabriel@optica.csic.es (Gabriel Cristóbal), boris@servidor.unam.mx (Boris Escalante-Ramírez)

tion and noisy changes. In the experiments we have considered two different databases: Brodatz and CURET for different sizes of LBP masks. Experimental results demonstrated the effectiveness and robustness of the described texture descriptors for images that are subjected to geometric or radiometric changes.

Keywords: Classification, Distance Measure, Invariant Descriptor, Local Binary Pattern, Texture Analysis

1. Introduction

Texture is the term used to characterize object surfaces and is used for pattern identification. It has been studied in the fields of visual perception and computer vision. Although it is a feature often used to characterize objects, it has been difficult to establish an appropriate definition. Since a texture is quite varied and can exhibit a large number of properties, many vision researchers have given definitions frequently in the context of different applications areas, Tuceryan and Jain (1998). However, from a mathematical point of view, it is usual to analyze textures as intensity variations from regularity –when textures simply contain periodic patterns– to randomness –where textures look like unstructured noise.

There are many ways to classify textures. Haralick (1979) proposed two different approaches: the statistical and the structural methods. The first one considers textures as the arrangement of spatial distribution of gray values in images. Inside of this group one can highlight the features extracted from the co-occurrence matrix, Davis et al. (1979). Structural methods are based on considering that textures are composed by primitives called “textons”. In

18 this direction, Wang and He (1990) introduced a model where textures can
19 be characterized by its texture spectrum, a set of essential small units.

20 A more detailed texture classification was later proposed by Paget (2008),
21 the approaches may be divided into the following categories: *i*) **statistical**
22 **methods:** a set of features is used to represent textures. The basic as-
23 sumption is that the intensity variations are more or less constant within
24 a texture region and takes a greater value outside its boundary. Statistical
25 measures analyze spatial distribution of pixels using features extracted from
26 the first and second-order histogram statistics Guo et al. (2010b). *ii*) **spec-**
27 **tral methods:** these methods collect a distribution of filter responses as
28 input to further classification or segmentation. In particular, Gabor filters
29 have proven to be powerful and precise for describing texture patterns, Nava
30 et al. (2011). Novel approaches seem to lead towards an improvement of Ga-
31 bor filters by using local binary patterns as a complementary tool to extract
32 texture features as in Ma and Zhu (2007); Nguyen et al. (2009); Zhang et al.
33 (2005). Many algorithms in this category are focusing on face recognition,
34 Huang et al. (2011). In addition, a recent analysis of rotational invariant
35 texture features appears in Estudillo-Romero and Escalante-Ramirez (2011).
36 *iii*) **structural methods:** some textures can be viewed as two dimensional
37 patterns consisting of a set of primitives which are arranged according to
38 a certain placement rules. *iv*) **stochastic methods:** textures are assumed
39 to be the realization of a stochastic process. The parameter estimation as-
40 sociated with the process is quite complicated although there are good ap-
41 proaches in the literature, e.g., Seetharaman (2009) use a Bayesian approach
42 as a texture descriptor.

43 Texture analysis through a LBP operator can be considered as a combina-
44 tion of both statistical and structural methods. Therefore, it can be expected
45 a good LBP performance in a wide variety of texture identification scenarios.
46 LBP constitutes an image operator that transforms an image into an array of
47 integer labels that encode the pixel-wise information of the texture images.
48 These labels can be represented as a histogram that can be interpreted as
49 the fingerprint of the analyzed object. In fact, the LBP approach belongs to
50 a group of non-local parametric transformations that is distinguished by the
51 use of ordering information among data, rather than the data values them-
52 selves. Non-parametric local transformations are local image transformations
53 that rely on the relative ordering of the intensity values.

54 Similarly to the Ojala et al. (1994) work, Zabih and Woodfill (1994) pro-
55 posed two alternative non-parametric local transforms. The first transform
56 called rank transform (RT) is defined as the number of pixels in a local square
57 region whose values are lesser that the value of a central pixel. The second
58 non-parametric local transform named census transform (CT) maps the local
59 square neighborhood into a bit string representing the set of neighbor pixels
60 whose intensities are lesser than a central pixel value. Both RT and CT de-
61 pend solely on a set of pixel comparisons. The first limitation of these kind
62 of methods is that the amount of information associated to a pixel is not
63 very large which induces noise sensitivity. Another limitation is that the lo-
64 cal measures rely heavily upon the intensity of a central pixel. Nevertheless,
65 the last drawback is not an issue by doing comparisons using local means or
66 median values instead of central pixel intensities Zabih and Woodfill (1994).

67 After the initial LBP proposal, many modifications and improvements

68 have emerged in the literature, most of them are related to face analysis
69 where it is assumed that input faces are registered. For this reason, many
70 modifications are not invariant to rotational transforms. For a thorough
71 description of LBP operators see two recent surveys and a book monograph:
72 Nanni et al. (2011); Huang et al. (2011); Pietikäinen et al. (2011).

73 This paper is organized as follows. Section 2 presents an overview of LBP
74 methods as well as the most significant extensions that have been proposed
75 to obtain rotational invariance. In Section 3 an exhaustive evaluation of
76 different LBP approaches previously mentioned as well as a comparative
77 analysis of LBP rotational invariant proposals is shown. This study includes
78 a few tests with noise and illumination changes using a rotated version of the
79 Brodatz database, Brodatz (1966) and the CURET texture database, Dana
80 et al. (1999). Finally our work is summarized in Section 4.

81 **2. Local Binary Pattern Overview**

82 The very first approach to LBP was given in Ojala et al. (1994). Ojala
83 proposed a two-level version of the original method of Wang and He (1990).
84 Ojala claimed that this refinement provides a robust way for describing local
85 texture patterns. However, very recently Tan and Triggs (2010) have revis-
86 ited the original approach and demonstrated that a generalization of LBP
87 called local ternary patterns (LTP) is more discriminant and less sensitive to
88 noise for texture analysis.

89 The simple LBP uses a 3×3 square mask called “texture spectrum”
90 that represents the neighborhood around a central pixel, (see Fig. 1(a)).
91 The values of the neighbor pixels within the square mask are thresholded

92 by the value of their central pixel. Pixel values under the threshold are
 93 labeled with “0” otherwise they are labeled with “1”, Fig. 1(b). The labeled
 94 pixels are multiplied by a weight function according with their positions,
 95 Fig. 1(c). Finally, the values of the eight pixels are summed to obtain a
 96 label for this neighborhood, Fig. 1(d). This method produced 2^8 possible
 97 labels. After this process is completed for the whole image, a label or LBP
 98 histogram is computed so that can be interpreted as a fingerprint of the
 99 analyzed object. Although this method provides information about local
 100 spatial structures, it is not invariant to rotational changes and does not
 101 include contrast information which has been demonstrated to be crucial to
 102 improve the discrimination of some textures.

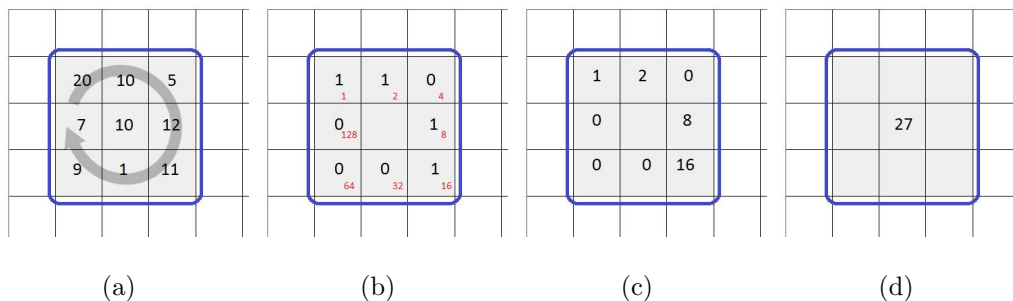


Figure 1: Based on a square mask of 3×3 the LBP algorithm computes the label by comparisons between central pixels and their surrounding neighbors.

103 The classic LBP operator was later generalized by Ojala et al. (2002).
 104 Such generalization can be obtained using a circular neighborhood denoted
 105 by (P, R) where P represents the number of sampling points and R rep-
 106 represents the radius of the neighborhood. The sampling point coordinates
 107 (x_p, y_p) are calculated using the formula $(x_c + R \cos(\frac{2\pi p}{P}), y_c - R \sin(\frac{2\pi p}{P}))$.
 108 When sampling coordinates do not fall at integer positions, the intensity

109 value is bilinearly interpolated. This implementation is called interpolated
 110 LBP ($LBP_{P,R}$).

111 $LBP_{P,R}$ is defined as an ordered set of binary comparisons of pixel inten-
 112 sities between a central pixel and its surrounding neighbors as follows:

$$LBP_{P,R}(g_c) = \sum_{p=0}^{P-1} s(g_p - g_c) 2^p \quad (1)$$

113 where g_c is the intensity value of the central pixel at (x_c, y_c) coordinates and
 114 $\{g_p | p = 0, \dots, P - 1\}$ is the intensity value of the p -neighbor. The thresh-
 115 olding function $s(x)$ is defined as:

$$s(x) = \begin{cases} 1 & \text{if } x \geq 0 \\ 0 & \text{if } x < 0 \end{cases} \quad (2)$$

116 Eq. (1) represents a texture unit composed of $P + 1$ elements (central
 117 pixel included). In total, there are 2^P possible texture units describing spatial
 118 patterns in a neighborhood of P points. $LBP_{P,R}$ achieves invariance against
 119 any monotonic transformation by considering the sign of the differences in
 120 $s(g_p - g_c)$, which effectively corresponds to binary thresholding of the local
 121 neighborhood.

122 $LBP_{P,R}$ is defined on a circular neighborhood allowing to change the
 123 number of neighbors and the radius size. However, increasing the number
 124 of neighbors increases the information redundancy and the computational
 125 cost, which not always resulting in a more discriminant LBP label. In this
 126 direction, Liao and Chung (2007) defined the elongated LBP (ELBP) based
 127 on an anisotropic neighborhood allowing to improve texture discrimination
 128 by implementing multi-orientation analysis.

129 In relation with the size of the radius, Liao et al. (2007) proposed a
 130 representation called multi-scale block LBP (MBLBP). The computation is
 131 done based on averaging values of block subregions instead of individual
 132 pixels. In this paper will further analyze the influence of the neighborhood
 133 size, (see Fig. 2).

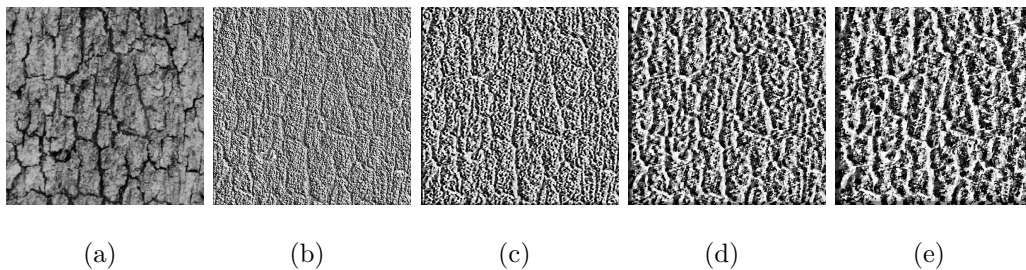


Figure 2: LBP depends solely on the set of ordered comparisons between a central pixel and its surrounding neighbors. Specifically, $LBP_{P,R}$ allows to analyze neighborhoods with different sizes and number of neighbors. Nonetheless, the larger neighborhood size the coarse LBP image become. LBP images from Fig. 2(b) to Fig. 2(c) are texture processed by the LBP operator with different values of P and R . 2(a) Bark texture (D12). 2(b) $P = 8, R = 1$. 2(c) $P = 8, R = 5$. 2(d) $P = 8, R = 10$. 2(e) $P = 1, R = 15$.

134 Under a rotational transform the values of $\{g_p | p = 0, \dots, P - 1\}$ will move
 135 along a circular path around a central pixel g_c resulting into different labels.
 136 Pietikäinen et al. (2000) proposed a modification called rotational invariant
 137 LBP ($LBP_{P,R}^{min}$) to remove the rotational effects by labeling each rotation
 138 with an identifier as follows:

$$LBP_{P,R}^{min}(g_c) = \min \{ROR(LBP_{P,R}(g_c), i) | i = 0, \dots, P - 1\} \quad (3)$$

139 where $ROR(x, i)$ performs a circular bitwise right shift operation i times.

140 The main idea is to rotate the P neighbors to find the minimum value
 141 that the neighbor chain may represents. This approach identifies 36 different

142 values when using $P = 8$. Nevertheless, Eq. (3) achieves invariance only for
 143 a discrete digital domain because only for 90° perfect rotational invariance
 144 can be attained.

145 Ojala et al. (2002) observed that over 90% of LBPs entail fundamental
 146 properties of textures that can be described with very few spatial transitions.
 147 He introduced a uniformity measure $U(LBP_{P,R}(g_c))$ which corresponds to
 148 the number of spatial transitions in the pattern as follows:

$$U(LBP_{P,R}(g_c)) = |s(g_{p-1} - g_c) - s(g_0 - g_c)| + \sum_{p=1}^{P-1} |s(g_p - g_c) - s(g_{p-1} - g_c)| \quad (4)$$

149 in this way the so-called uniform LBP ($LBP_{P,R}^{uni}$) can be obtained as:

$$LBP_{P,R}^{uni}(g_c) = \begin{cases} \sum_{p=0}^{P-1} s(g_p - g_c) & \text{if } U(LBP_{P,R}(g_c)) \leq 2 \\ P + 1 & \text{otherwise} \end{cases} \quad (5)$$

150 Eq. (5) represents a gray-scale and rotational invariant texture descriptor
 151 that assigns a unique label to each patterns where the number of spatial
 152 transitions is at most two. These labels corresponding to the number of
 153 “1” in the pattern chain while the rest of the non-uniform patters (where
 154 the number of spatial transitions is greater than two) are grouped under the
 155 label $P + 1$. The discrete histogram of the uniform patterns obtained has
 156 been shown to be a very powerful feature for characterizing textures, Zhou
 157 et al. (2008).

158 2.1. Modifications of rotational invariant LBP

159 In Eq. (5) all patterns are divided according with the number of spatial
 160 transitions resulting in $P + 1$ sets of uniform patterns. One disadvantage is
 161 that patterns with more that two transitions are grouped into a unique label

162 which leads to loss of discrimination. The reason for that due to the fact
 163 there not exists a general pattern that will be able to describe all textures.
 164 Every pattern is well suited for describing just a certain texture. Ma (2011)
 165 proposed the number LBP ($LBP_{P,R}^{num}$) as an extension of the $LBP_{P,R}^{uni}$ by
 166 dividing the non-uniform patterns into groups based on the number of “1”
 167 bits or “0” bits as follows:

$$LBP_{P,R}^{num}(g_c) = \begin{cases} \sum_{p=0}^{P-1} s(g_p - g_c) & \text{if } U(LBP_{P,R}(g_c)) \leq 2 \\ Num_1\{LBP_{P,R}(g_c)\} & \text{if } U(LBP_{P,R}(g_c)) > 2 \text{ and} \\ & Num_1\{LBP_{P,R}(g_c)\} \geq Num_0\{LBP_{P,R}(g_c)\} \\ Num_0\{LBP_{P,R}(g_c)\} & \text{if } U(LBP_{P,R}(g_c)) > 2 \text{ and} \\ & Num_1\{LBP_{P,R}(g_c)\} < Num_0\{LBP_{P,R}(g_c)\} \end{cases} \quad (6)$$

168 where $Num_1\{\bullet\}$ is the number of “1” and $Num_0\{\bullet\}$ is the number of “0” in
 169 the non-uniform pattern.

170 Along the same direction, Zhou et al. (2008) proposed an extension by di-
 171 viding the non-uniform patterns according to their structural properties and
 172 merging them on the basis of their degree of similarity so that the final his-
 173 togram reflects texture information more efficiently because it may represent
 174 the stochastic components of textures. Moreover, Ma (2011) outperforms
 175 Zhou’s results.

176 Liu et al. (2011) stated that the probability of a central pixel depends
 177 only on its neighbors. In this way the neighbor intensity LBP ($LBP_{P,R}^{ni}$)
 178 can be defined by replacing the central pixel value with the average of its
 179 neighbors as follows:

$$LBP_{P,R}^{ni}(g_c) = \sum_{p=0}^{P-1} s(g_p - \mu)2^p \quad (7)$$

180 where

$$\mu = \frac{1}{p} \sum_{p=0}^{p-1} g_p \quad (8)$$

181 The presence of noise in images can seriously impair the texture extraction
182 performance of the LBP operator. In this paper we propose to use the median
183 operator in order to reduce noise effects. Such proposal replace the central
184 pixel value with the median of itself and the P neighbors as follows:

$$LBP_{P,R}^{med}(g_c) = \sum_{p=0}^{p-1} s(g_p - \tilde{g}) \quad (9)$$

185 where \tilde{g} represents the median of the p neighbors and the central pixel, Zabih
186 and Woodfill (1994). This LBP modification is still invariant to rotation but
187 less sensitive to noise. It is also invariant to monotonic illumination changes.

188 *2.2. Other LBP extensions oriented to face analysis*

189 In the last few years, face image analysis has been one of the most active
190 research areas where LBP has been exploited because its effectiveness in deal
191 with various challenging task of face analysis. Since most of the face detection
192 or segmentation algorithms include a normalization step –which means that
193 faces are registered– as a preprocessing step and therefore the LBP methods
194 do not need to present affine invariant features.

195 Fu and Wei (2008) addressed the problem of noise sensitivity by consid-
196 ering that in most cases central pixels provide more information than their
197 neighbor counterparts, so they assigned to the central pixels a bigger weight.
198 In the case of images degraded by white noise Fu and Wei considered a

199 modified version of Eq. (2) as:

$$s(x) = \begin{cases} 1 & |x| \geq c \\ 0 & |x| < c \end{cases} \quad (10)$$

200 where c is a fixed threshold.

201 In summary, Fu and Wei considered that central pixels are more impor-
 202 tant than their neighbors and thus proposed the centralized LBP ($LBP_{P,R}^{cen}$)
 203 as follows:

$$LBP_{P,R}^{cen}(g_c) = \sum_{p=0}^{\frac{p}{2}-1} s\left(g_p - g_{p+\frac{p}{2}}\right) 2^p + s(g_c - g_{tot}) 2^{\frac{p}{2}} \quad (11)$$

204 and g_{tot} is defined as:

$$g_{tot} = \frac{1}{p+1} \left(g_c + \sum_{p=0}^{p-1} g_p \right) \quad (12)$$

205 where g_c and (x_c, y_c) represent the intensity and coordinates of the central
 206 pixel respectively. Due to the fact that the algorithm considers correlation
 207 between opposite pixel points, this algorithm is not rotational invariant.

208 Tan et al. (2010) proposed an extension to the operator, Eq. (1), called
 209 extended LBP ($LBP_{P,R}^{ext}$) by using the value of central pixels plus a tolerance
 210 interval t as local threshold, t is a user-specific value, usually set at “1”. Each
 211 pixel value within the interval zone $g_c \pm t$ is quantized as zero. Pixel values
 212 above the tolerance interval are labeled with “1” and those below this zone
 213 are labeled with “-1” as follows:

$$s(x) = \begin{cases} 1 & \text{if } x > t \\ 0 & \text{if } |x| \leq t \\ -1 & \text{if } x < -t \end{cases} \quad (13)$$

214 here x is the difference between the P neighbors and their central pixels.
 215 Each ternary pattern is split into upper and lower pattern and each part
 216 is encoded as a separate LBP pattern. Finally, their LBP histograms are
 217 concatenated.

218 Guo et al. (2010a) suggested using both the sign and magnitude of a
 219 d_p vector to form the so-called completed LBP ($LBP_{P,R}^{com}$). In Eq. (1) only
 220 the sign component is considered whereas in the Guo et al. proposal, $d_p =$
 221 $\{g_p - g_c | p = 0, 1, \dots, P - 1\}$ is split into two components as follows:

$$d_p = s_p * m_p = \begin{cases} s_p & = \text{sign}(d_p) \\ m_p & = |d_p| \end{cases} \quad (14)$$

222 where s_p and m_p are the sign and magnitude of d_p respectively. In addition,
 223 they presented an analysis of the sign component and concluded that s_p
 224 preserves more information of d_p than m_p . They defined three operators that
 225 are combined to build the LBP histogram: $LBP_{S,P,R}^{com}$, which considers the sign
 226 component of d_p , $LBP_{C,P,R}^{com}$ which considers the magnitude component of d_p ,
 227 and $LBP_{C,P,R}^{com}$ which considers the magnitude of central pixels.

228 Finally, Liao et al. (2009) proposed the dominant LBP ($LBP_{P,R}^{dom}$) which
 229 is a modification of Eq. (5) based on the fact that $LBP_{P,R}^{uni}$ in practice is not
 230 well suited to encode some complicated pattern textures such as curvature
 231 edges and crossing boundaries of corners. A possible explanation is due to the
 232 fact that the extracted uniform patterns do not have a dominant proportion
 233 of them to better represent the object (or image). Liao et al. have shown
 234 that given a set of training images, the required number of patterns to better
 235 representing textures corresponds to at least 80% of the pattern occurrences.
 236 The first step of their procedure is to compute the LBP histogram and sort

237 it in descending order. The second step is to extract a vector for obtain 80%
238 of pattern occurrences. This procedure guarantees a suitable framework for
239 representing textures.

240 2.3. LBP histogram evaluation

241 Since LBP operators act as fingerprint of texture, it is possible to use
242 LBP histogram distances as a similarity measure among all different textures.
243 Two different methodologies can be used for histogram distance evaluation:
244 vector and probabilistic approaches. In the vector approach, a histogram
245 is treated as a fixed-dimensional vector. Hence standard vector norms such
246 as city block or Euclidean between univariate histograms can be used. The
247 probabilistic approach is based on the fact that a histogram provides the
248 basis for an empirical estimation of the probabilistic density function (pdf).
249 Computing the distance between two histograms is equivalent to measure the
250 overlapping part between two pdf's as the distance.

251 Although the Kullback-Leibler divergence (KL) –a generalization of Shan-
252 non's entropy– is not a true metric rather it is a relative entropy, it can be
253 used as a suitable metric for measuring distances between histograms as fol-
254 lows:

$$D_{KL}(A, B) = \sum_{i=0}^{b-1} P_i(B) \log \frac{P_i(B)}{P_i(A)} \quad (15)$$

255 where A and B are two histograms with b bins length each, and P_i denotes
256 the probability of the bin i .

257 Cha and Srihari (2002) proposed a novel histogram distance measure
258 called ordinal distance (OD) based on the idea that a histogram $h(A)$ can
259 be transformed into a histogram $h(B)$ by moving elements from left to right,

260 being the total movements the distance between them.

$$D_{ord} \{h(A), h(B)\} = \sum_{i=0}^{b-i} \left| \sum_{j=0}^i (h_j(A), h_j(B)) \right| \quad (16)$$

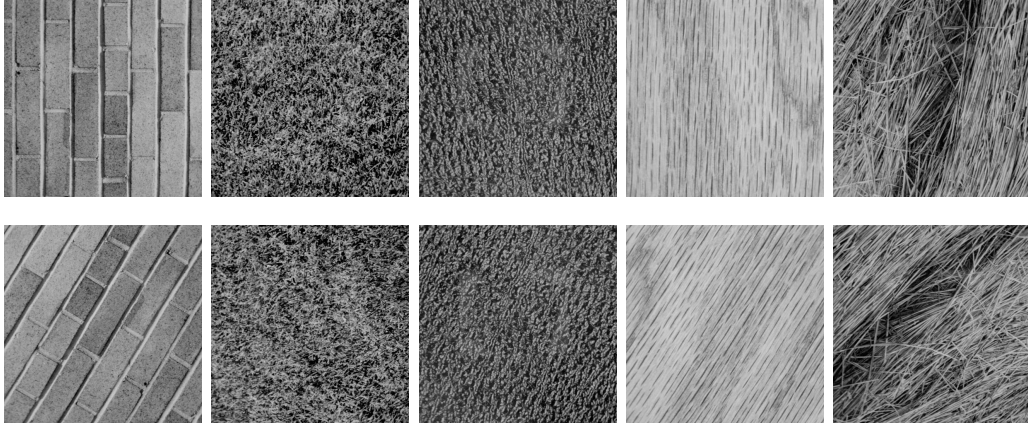
261 In the next Section 3, we present several experiments of texture classifi-
262 cation using both KL and OD metrics in order to compare the performance
263 of seven LBP approaches under several settings.

264 3. Experiments and results

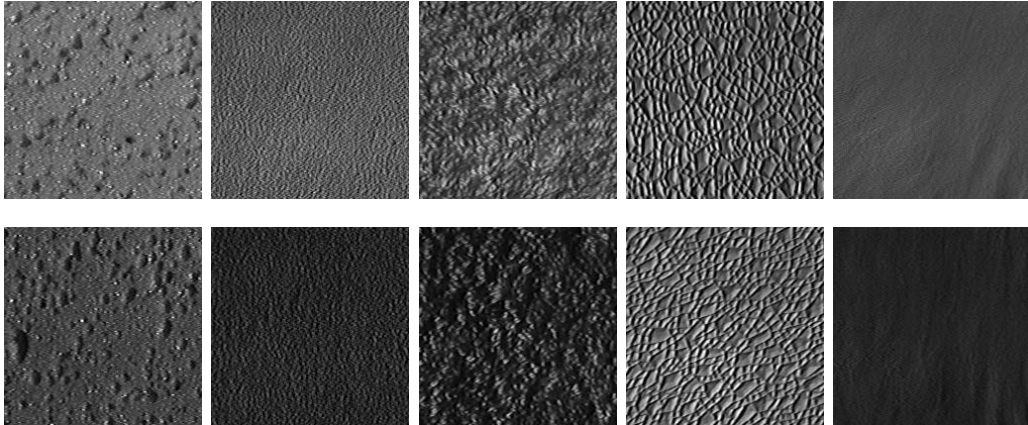
265 We split experimental assessments into three categories: rotational, noisy,
266 and illumination changes. The first two evaluations were performed using the
267 USC-SIPI image database available at Brodatz. This database is a rotated
268 version of Brodatz database and consists of thirteen images each digitized at
269 seven different rotation angles: 0, 30, 60, 90, 120, 150, and 200 degrees. The
270 images are all 512×512 pixels with 8 bits/pixel, see Fig. 3(a).

271 For illumination tests we used a large enough subset of the CURET
272 database, available at Dana et al., to validate our experiments. In the last
273 case, we employed ten reference images with ten illumination variations each
274 for a total of 100 images; the images are all 200×200 pixels and were con-
275 verted into gray scale with 8 bits/pixel, see Fig. 3(b). The classification
276 procedure setup consisted of comparing LBP histogram distances of each
277 reference image against the test images.

278 In order to evaluate the performance of the previously described seven ro-
279 tational invariant LBP approaches, we used the next thirteen textures as ref-
280 erence images: bark (D12), brick (D94), bubbles (D112), grass (D9), leather
281 (D24), pigskin (D92), raffia (D84), sand (D29), straw (D15), water(D38),



(a)



(b)

Figure 3: 3(a) The first row shows five reference images: brick (D94), grass (D9), leather (D24), wood (D68), and straw (D15), the second row shows the rotated versions of the reference images, (150°). 3(b). The third and the fourth rows present a subset of images from the CURET database.

282 weave (D16), wood (D68), and wool (D19) -the number between parenthesis
 283 is the identification number in the Brodatz texture book, Brodatz (1966).
 284 We measured and compared distances among all histograms (71 rotated tex-
 285 tures and 13 reference textures) using the two metrics previously presented
 286 in Eq. (15) and Eq. (16) and we assigned a rotated image to a certain tex-
 287 ture according to the closest distance between LBP histograms. See Table 1
 288 for comparative study of the accuracy performance. In addition we used
 289 confusion matrices to obtained the accuracy rate (AR) of the seven LBP
 290 approaches using the next equation:

$$AR = \left(\frac{\sum_i^k a_{i,i}}{\sum_{i,j}^k a_{i,j}} \right) \times 100\% \quad (17)$$

291 where (i, j) are matrix indexes and k is the number of texture references.

Table 1: Comparison of seven LBP approaches. LBP^{min} and $LBP_{P,R}^{min}$ differ that the first one does not use interpolated neighbors but the second one does.

Scheme	OD metric		KLD metric		Reference
	# textures	Accuracy rate (%)	# textures	Accuracy rate (%)	
LBP	35	38.46	39	42.86	Ojala et al. (1994).
LBP^{min}	79	86.81	84	92.31	Ojala et al. (1994).
$LBP_{P,R}^{min}$	77	84.62	72	74.00	Pietikäinen et al. (2000).
$LBP_{P,R}^{uni}$	80	87.91	82	90.11	Ojala et al. (2002).
$LBP_{P,R}^{num}$	83	91.21	80	87.91	Ma (2011).
$LBP_{P,R}^{ni}$	76	83.52	74	81.32	Liu et al. (2011).
$LBP_{P,R}^{med}$	72	79.12	64	70.33	Zabih and Woodfill (1994).

292 Original Ojala’s proposal achieved the lowest AR because is not invariant
 293 to rotation with 35 out of 91 textures correctly classified in the worst scenario.
 294 Although this paper is focused to analyze invariant to rotation approaches, we

295 performed a comparison between LBP and $LBP_{P,R}^{cen}$, (see Eq. 11). $LBP_{P,R}^{cen}$
 296 achieved an AR of 29.61% using the OD metric and 36.26% of textures
 297 correctly classified under the KL metric. $LBP_{P,R}^{cen}$ performance was even
 298 lower than original Ojala’s proposal. One of the possible reasons is that
 299 $LBP_{P,R}^{cen}$ uses a fixed threshold c in Eq. (10) which influences the accuracy
 300 rate.

301 On the other hand, $LBP_{P,R}^{num}$ achieved 91.91% of textures correctly clas-
 302 sified, 3.3% more than $LBP_{P,R}^{uni}$ with 87.91%. This can be interpreted as
 303 $LBP_{P,R}^{num}$ add extra information of non-uniform patterns into the LBP his-
 304 togram whereas $LBP_{P,R}^{uni}$ labels all non-uniform patterns into a unique label
 305 which discards the large amount of texture information represented by these
 306 patterns. Another possible explanation is that stochastic components are dis-
 307 regarded when all non-uniform patterns are grouped because they represent
 308 abrupt variations and changes in the textures.

309 Table 2 and Table 3 present the best AR in the form of confusion matrices
 310 for the OD and KLD metrics respectively.

311 From Table 3 one can observe that LBP^{min} provides the higher rate using
 312 the KL metric. Since KL metric is a measure of relative entropy, there is a
 313 strong suspicious that when neighbors are calculated by bilinear interpola-
 314 tion, extra information is added which increases the distance between LBP
 315 histograms affecting the classification.

316 We compared the performance of LBP^{min} , $LBP_{P,R}^{min}$, $LBP_{P,R}^{uni}$, $LBP_{P,R}^{num}$,
 317 $LBP_{P,R}^{ni}$, and $LBP_{P,R}^{med}$ in terms of accuracy using $P = 8$ and $R = 1$ on
 318 a circular neighborhood, (see Fig. 4). This configuration has shown good
 319 results in discriminating similar textures. We computed a set of OD and KLD

Table 2: Confusion matrix for the classification experiment of $LBP_{P,R}^{num}$ using OD metric. Major mistakes occurred between grass (D9) and leather (D24) textures and between wood (D68) and straw (D15) textures.

		Predicted											
		bark	brick	bubbles	grass	leather	pigskin	raffia	sand	straw	water	weave	wood
Actual	bark	7	0	0	0	0	0	0	0	0	0	0	0
	brick	0	7	0	0	0	0	0	0	0	0	0	0
	bubbles	0	0	7	0	0	0	0	0	0	0	0	0
	grass	0	0	0	4	3	0	0	0	0	0	0	0
	leather	0	0	0	0	7	0	0	0	0	0	0	0
	pigskin	0	0	0	0	0	7	0	0	0	0	0	0
	raffia	0	0	0	0	0	0	7	0	0	0	0	0
	sand	2	0	0	0	0	0	0	7	0	0	0	0
	straw	0	0	0	0	0	0	0	0	7	0	0	0
	water	0	0	0	0	0	0	0	0	0	7	0	0
	weave	0	0	0	0	0	0	0	0	0	0	7	0
	wood	0	0	0	0	0	0	0	0	5	0	0	2
	wool	0	0	0	0	0	0	0	0	0	0	0	7

Table 3: Confusion matrix for the classification experiment of LBP^{min} using KLD metric. Most mistakes occurred when rotated wool textures were classified as straw texture. On the contrary, all the rotated straw textures were correctly classified.

		Predicted												
		bark	brick	bubbles	grass	leather	pigskin	raffia	sand	straw	water	weave	wool	wood
Actual	bark	7	0	0	0	0	0	0	0	0	0	0	0	0
	brick	0	7	0	0	0	0	0	0	0	0	0	0	0
	bubbles	0	0	7	0	0	0	0	0	0	0	0	0	0
	grass	0	0	0	6	1	0	0	0	0	0	0	0	0
	leather	0	0	0	0	7	0	0	0	0	0	0	0	0
	pigskin	0	0	0	0	0	7	0	0	0	0	0	0	0
	raffia	0	0	0	0	0	0	7	0	0	0	0	0	0
	sand	0	0	0	0	0	0	0	7	0	0	0	0	0
	straw	0	0	0	0	0	0	0	0	7	0	0	0	0
	water	0	0	0	0	0	1	0	0	0	6	0	0	0
	weave	0	0	0	0	0	0	0	0	0	0	7	0	0
	wool	0	0	0	0	0	0	0	0	5	0	0	2	0
	wood	0	0	0	0	0	0	0	0	0	0	0	0	7

320 values by compared each reference image in the database with its rotated
321 versions. Thus the most accurate technique is the one that brings the smallest
322 mean. We followed the assessment methodology proposed in Orjuela et al.
323 (2011) by quantifying the distance between distinctive textures using both
324 OD and KL metrics, Fig. 4(a) and Fig. 4(b) respectively.

325 Since the seven LBP approaches are rotational invariant is expected that
326 distances are to be zero or close to zero but due to the fact that the rotated
327 textures were scanned using a 512×512 pixel video digitizing camera, the
328 CCDs may has introduced some values that produce higher distances among
329 LBP histograms.

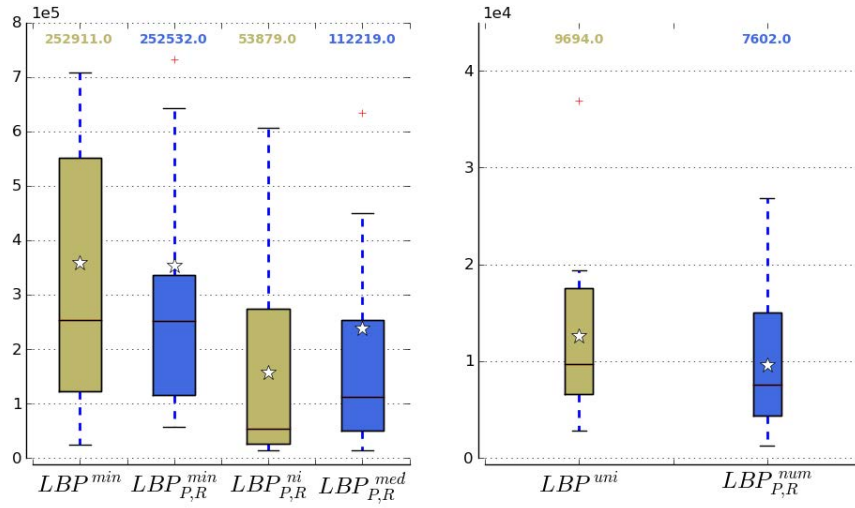
330 *3.1. Neighborhood size*

331 An important issue of original LBP is the neighborhood size. It has
332 small spatial support area, hence the bit-wise therein made between two
333 single intensity value pixels is affected by noise. The next experiment was
334 aimed to assess the radius size influence in texture classification. We present
335 the classification performance of five LBP approaches with different radius
336 $R = \{1, 2, 3\}$.

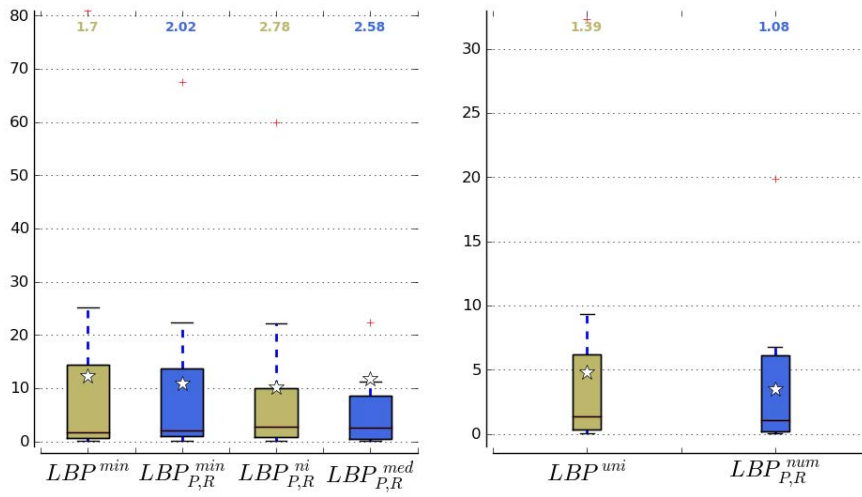
337 Fig. 5 shows the classification performance comparison among five LBPs.
338 In all cases the highest classification rate was achieved with $R = 2$. On the
339 contrary, the increased size of the radius caused a poor classification rate
340 starting from $R = 3$.

341 *3.2. Noise*

342 LBP approaches are very sensitive to noise specially when a small neigh-
343 borhood is used. Since the amount of information associated to a pixel is



(a)



(b)

Figure 4: Fig. 4(a) mean distances using OD metric. Fig. 4(b) mean distances using KL metric.

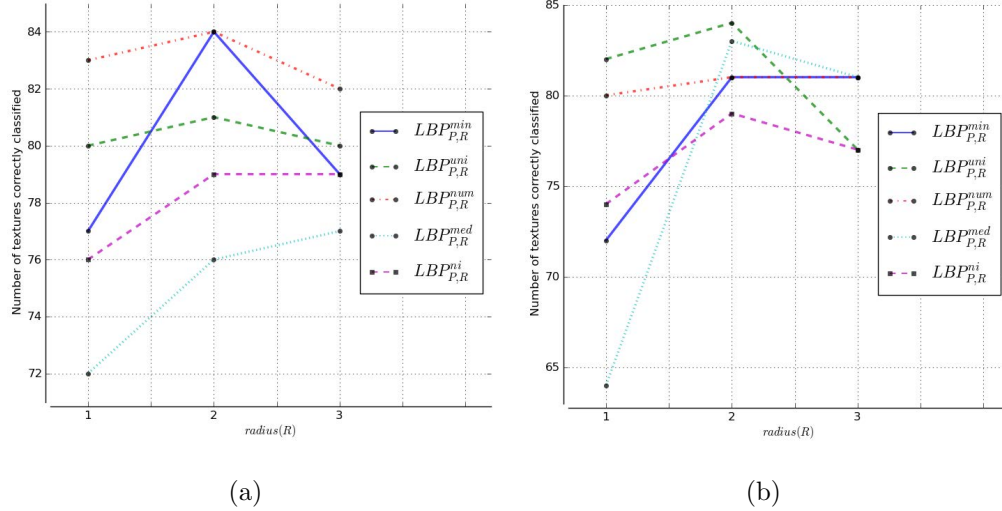


Figure 5: AR of the LBP approaches using different radius sizes $R = \{1, 2, 3\}$. Fig. 5(a) OD metric. Fig. 5(b) KL metric.

344 not very large, even a small pixel value change due to noise could lead to
 345 a different LBP label. Fig. 6 presents the accuracy rate of LBPs under the
 346 influence of additive Gaussian noise using OD metric. In this experiment we
 347 used the USC-SIPI database described in the preceding section. Gaussian
 348 noise with $\mu = 0$ and $\sigma^2 = 0.06$ was added to the image database. This
 349 addition was implemented using Matlab *imnoise* function.

350 Since Gaussian noise affects the AR, LBP demands to use preprocessing
 351 denoising step or normalization stage in order to avoid noise artifact influence.

352 3.3. Illumination

353 Lighting variation is one of the major challenge for the current feature
 354 descriptors. Tan and Triggs (2010) presented a study of texture analysis
 355 under difficult lighting conditions and claims that LBP performance decreases
 356 almost exponentially under extreme illumination conditions. LBP by itself

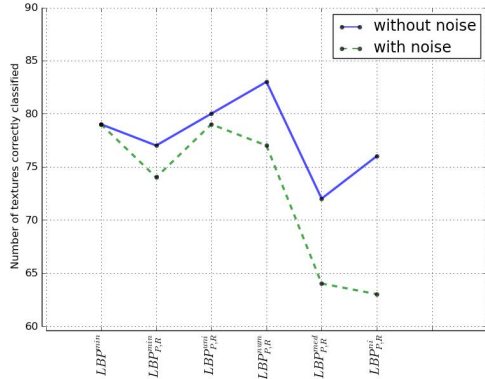


Figure 6: Performance of LBP approaches under additive Gaussian noise with media $\mu = 0$ and $\sigma^2 = 0.06$.

357 is not invariant to illumination changes and does not address the contrast of
 358 textures which is important in the discrimination. For this purpose, we are
 359 interested in combined LBP operators with a contrast information measure
 360 (CI), Eq. (18). However, CI produces continuous values which need to be
 361 quantized. Ojala et al. (1994) proposed to quantize contrast values so that
 362 all bins have an equal number of elements. So far, setting the number of bins
 363 is still an open issue.

364 LBP and CI histograms could be combined in two ways: jointly or hy-
 365 bridly, Guo et al. (2010a). In the first one, similar to 2D joint histograms, we
 366 can build a 3D joint histogram of them. In the second way, a large histogram
 367 is built by concatenating both LBP and CI histograms to form the so-called
 368 “pseudo joint histogram”.

$$CI = \sum_{i=0}^{m-1} G_i - \sum_{i=0}^{n-1} g_i \quad (18)$$

369 where G_i are the m neighbor pixels greater or equals than g_c and g_i are the
 370 n neighbor pixels lesser than g_c .

371 In the next experiment we performed classification of textures under dif-
 372 ferent illumination conditions using the CURET database.

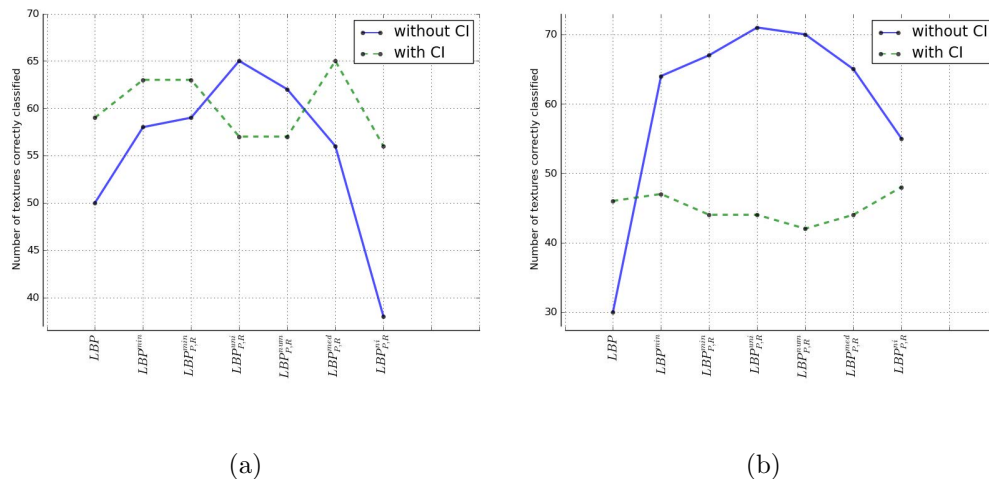


Figure 7: Texture classification under illumination changes. Fig. 7(a) shows performance of seven LBP/CI approaches using the OD metric. Fig. 7(b) shows performance of seven LBP/CI approaches using the KL metric

373 As we expected, the AR achieved are lower than the results presented for
 374 rotational invariant analysis because LBP methodology is not illumination
 375 invariant. Nevertheless, CI improved the AR of almost every LBP meth-
 376 ods using OD metric except for those methods based on uniform patterns,
 377 where their LBP histogram contains $P + 1$ bins. In these cases, we need to
 378 apply other methodologies that are out of the scope of this study. On the
 379 contrary, in Fig. 7(b) CI decreases the classification performance. A possi-
 380 ble explanation is that CI entropy influences negatively KL metric leading a

381 misclassification.

382 The combination of LBP and CI performs well in the case of rotational
383 cases too. For rotational invariant experiments, the AR of original *LBP*
384 using the USC-SIPI image database are 38.46% and 42.86% for OD and KL
385 metrics respectively. However, the AR increased up to 76.92% and 78.02%
386 for OD and KL metrics respectively by adding CI histograms.

387 4. Conclusions

388 LBP descriptors have been powerful tools for feature encoding. They
389 have been successfully used in many different image analysis applications, in
390 particular in the area of face recognition due to their excellent properties and
391 computational simplicity. Since original LBP proposal has many limitations
392 such as noise sensibility and it is affected by rotational transforms, a large
393 number of extensions have been proposed. We have presented a LBP state of
394 art for invariant and non-invariant rotational approaches. We evaluated the
395 performance of several LBP algorithms proposed in the literature for texture
396 classification. The results can be summarized into three groups: *i*) LBPs
397 based on minimal chains: LBP^{min} and $LBP_{P,R}^{min}$ compute a minimal chain.
398 Their performance could be affected by noise because if a pixel intensity
399 value is disturbed the final LBP label changes. *ii*) LBPs based on neighbor-
400 hood values: Prior a LBP label computation, $LBP_{P,R}^{ni}$ and $LBP_{P,R}^{med}$ perform
401 a weighted average of neighboring pixels to minimize the effects of noise.
402 *iii*) LBPs based on uniform values: $LBP_{P,R}^{uni}$, $LBP_{P,R}^{num}$ compute a uniformity
403 measure prior LBP label computation which corresponds to the number of
404 spatial transitions in the pattern. Since $LBP_{P,R}^{num}$ add extra information of

405 non-uniform patterns into the LBP histogram it has a better texture clas-
406 sification performance than $LBP_{P,R}^{uni}$. Further work includes extending this
407 techniques by applying a preprocessing stage based on Gabor filtering for
408 increasing the robustness to illumination and noise degradations. Another
409 extension will be based on the use of FPGAs to reduce the computational
410 time.

411 **Acknowledgments**

412 This work has been partially supported by the following UNAM grants:
413 PAPIIT IN113611 and IXTLI IX100610 and by the Spanish Ministry of Sci-
414 ence and Technology under projects TEC2010-20307 and TEC2010-09834-E.

415 **References**

- 416 Brodatz, P., . USC-SIPI. [http://sipi.usc.edu/database/database.php?](http://sipi.usc.edu/database/database.php?volume=rotate)
417 `volume=rotate`. [Online; accessed 1-September-2011].
- 418 Brodatz, P., 1966. Textures; a photographic album for artists and designers.
419 Dover, New York.
- 420 Cha, S.H., Srihari, S.N., 2002. On measuring the distance between his-
421 tograms. *Pattern Recognition* 35, 1355–1370.
- 422 Dana, J.K., Van-Ginneken, B., Nayar, S.K., Koenderink, J.J., 1999. Re-
423 flectance and texture of real world surfaces. *ACM Transactions on Graph-*
424 *ics (TOG)* 18, 1–34.

- 425 Dana, K., Van-Ginneken, B., Nayar, S., Koenderink, J., . CURET. [http:](http://www.cs.columbia.edu/CAVE/software/curet/html/btfm.html)
426 [//www.cs.columbia.edu/CAVE/software/curet/html/btfm.html](http://www.cs.columbia.edu/CAVE/software/curet/html/btfm.html). [On-
427 line; accessed 1-September-2011].
- 428 Davis, L.S., Johns, S.A., Aggarwal, J.K., 1979. Texture analysis using gen-
429 eralized co-occurrence matrices. *IEEE Transactions on Pattern Analysis*
430 *and Machine Intelligence PAMI-1*, 251–259.
- 431 Estudillo-Romero, A., Escalante-Ramirez, B., 2011. Rotation-invariant tex-
432 ture features from the steered Hermite transform. *Pattern Recognition*
433 *Letters* 32, 2150–2162.
- 434 Fu, X., Wei, W., 2008. Centralized Binary Patterns embedded with image
435 euclidean distance for facial expression recognition, in: *4th International*
436 *Conference on Natural Computation*, pp. 115–119.
- 437 Guo, Z., Zhang, L., Zhang, D., 2010a. A completed modeling of Local Binary
438 Pattern operator for texture classification. *IEEE Transactions on Image*
439 *Processing* 19, 1657–1663.
- 440 Guo, Z., Zhang, L., Zhang, D., Zhang, S., 2010b. Rotation invariant texture
441 classification using adaptive LBP with directional statistical features, in:
442 *17th IEEE International Conference on Image Processing (ICIP)*, pp. 285–
443 288.
- 444 Haralick, R.M., 1979. Statistical and structural approaches to texture. *IEEE*
445 *Proc.* 67, 786–804.
- 446 Huang, D., Shan, C., Ardabilian, M., Wang, Y., Chen, L., 2011. Local Binary
447 Patterns and its application to facial image analysis: a survey. *IEEE*

- 448 Transactions on Systems, Man, and Cybernetics, Part C: Applications
449 and Reviews 41, 765–781.
- 450 Liao, S., Chung, A., 2007. Face recognition by using Elongated Local Binary
451 Patterns with average maximum distance gradient magnitude, in: Yagi, Y.,
452 Kang, S., Kweon, I., Zha, H. (Eds.), Computer Vision (ACCV). Springer
453 Berlin / Heidelberg. volume 4844 of *Lecture Notes in Computer Science*,
454 pp. 672–679.
- 455 Liao, S., Law, M.W.K., Chung, A.C.S., 2009. Dominant Local Binary Pat-
456 terns for texture classification. *IEEE Transactions on Image Processing*
457 18, 1107–1118.
- 458 Liao, S., Zhu, X., Lei, Z., Zhang, L., Li, S., 2007. Learning Multi-scale
459 Block Local Binary Patterns for face recognition, in: Lee, S.W., Li, S.
460 (Eds.), *Advances in Biometrics*. Springer Berlin/Heidelberg. volume 4642
461 of *Lecture Notes in Computer Science*, pp. 828–837.
- 462 Liu, L., Fieguth, P., Kuang, G., 2011. Generalized Local Binary Patterns
463 for texture classification, in: *Proceedings of the British Machine Vision*
464 *Conference*, BMVA Press. pp. 123.1–123.11.
- 465 Ma, L., Zhu, L., 2007. Integration of the optimal Gabor filter design and
466 Local Binary Patterns for texture segmentation, in: *IEEE International*
467 *Conference on Integration Technology*, pp. 408–413.
- 468 Ma, Y., 2011. Number Local binary Pattern: an extended Local Binary
469 Pattern, in: *International Conference on Wavelet Analysis and Pattern*
470 *Recognition (ICWAPR)*, pp. 272–275.

- 471 Nanni, L., Brahnam, S., Lumini, A., 2011. Survey on LBP based texture
472 descriptors for image classification. *Expert Systems with Applications* .
- 473 Nava, R., Escalante-Ramirez, B., Cristobal, G., 2011. A comparison study of
474 Gabor and log-Gabor wavelets for texture segmentation, in: 7th Interna-
475 tional Symposium on Image and Signal Processing and Analysis (ISPA),
476 pp. 189–194.
- 477 Nguyen, H., Bai, L., Shen, L., 2009. Local Gabor Binary Pattern whitened
478 PCA: a novel approach for face recognition from single image per person,
479 in: Tistarelli, M., Nixon, M. (Eds.), *Advances in Biometrics*. Springer
480 Berlin / Heidelberg. volume 5558 of *Lecture Notes in Computer Science*,
481 pp. 269–278.
- 482 Ojala, T., Pietikainen, M., Harwood, D., 1994. Performance evaluation of tex-
483 ture measures with classification based on Kullback discrimination of dis-
484 tributions, in: *Proceedings of the 12th International Conference on Pattern*
485 *Recognition - Conference A: Computer Vision Image Processing (IAPR)*,
486 pp. 582 –585 vol.1.
- 487 Ojala, T., Pietikäinen, M., Maenpaa, T., 2002. Multiresolution gray-scale
488 and rotation invariant texture classification with Local Binary Patterns.
489 *IEEE Transactions on Pattern Analysis and Machine Intelligence* 24, 971–
490 987.
- 491 Orjuela, S.A., Quinones, R., Ortiz-Jaramillo, B., Rooms, F., de Keyser, R.,
492 Philips, W., 2011. Improving textures discrimination in the Local Binary

- 493 Patterns technique by using symmetry & group theory, in: 17th Interna-
494 tional Conference on Digital Signal Processing (DSP), pp. 1–6.
- 495 Paget, R., 2008. Texture modeling and synthesis, in: Mirmehdi, M., Xie, X.,
496 Suri, J. (Eds.), Handbook of Texture Analysis. Imperial College Press, pp.
497 33–60.
- 498 Pietikäinen, M., Hadid, A., Zhao, G., Ahonen, T., 2011. Computer vision
499 using Local Binary Patterns. volume 40. Springer. 1st edition, xv, 207 p.
500 87 illus., 56 in color edition.
- 501 Pietikäinen, M., Ojala, T., Xu, Z., 2000. Rotation-invariant texture classifi-
502 cation using feature distributions. Pattern Recognition 33, 43–52.
- 503 Seetharaman, K., 2009. Texture analysis based on a family of stochastic
504 models, in: IEEE International Conference on Signal and Image Processing
505 Applications (ICSIPA), pp. 518–523.
- 506 Tan, T., Zhang, M., Liu, F., 2010. Face recognition using Extended Local
507 Binary Patterns and fuzzy information fusion, in: 7th International Con-
508 ference on Fuzzy Systems and Knowledge Discovery (FSKD), pp. 625–629.
- 509 Tan, X., Triggs, B., 2010. Enhanced local texture feature sets for face recog-
510 nition under difficult lighting conditions. IEEE Transactions on Image
511 Processing 19, 1635–1650.
- 512 Tuceryan, M., Jain, A., 1998. Texture analysis, in: The Handbook of Pattern
513 Recognition and Computer Vision, pp. 207–248.

- 514 Wang, L., He, D.C., 1990. Texture classification using texture spectrum.
515 Pattern Recognition 23, 905–910.
- 516 Zabih, R., Woodfill, J., 1994. Non-parametric local transforms for computing
517 visual correspondence, in: Proceedings of the third European conference
518 on Computer Vision (Vol. II), Springer-Verlag New York, Inc., Secaucus,
519 NJ, USA. pp. 151–158.
- 520 Zhang, W., Shan, S., Gao, W., Chen, X., Zhang, H., 2005. Local Gabor Bi-
521 nary Pattern histogram sequence (LGBPHS): a novel non-statistical model
522 for face representation and recognition, in: 10th IEEE International Con-
523 ference on Computer Vision (ICCV), pp. 786–791 Vol. 1.
- 524 Zhou, H., Wang, R., Wang, C., 2008. A novel extended Local-Binary-Pattern
525 operator for texture analysis. Inf. Sci. 178, 4314–4325.